



Supplement of

Continental-scale evaluation of a fully distributed coupled land surface and groundwater model, ParFlow-CLM (v3.6.0), over Europe

Bibi S. Naz et al.

Correspondence to: Bibi S. Naz (b.naz@fz-juelich.de)

The copyright of individual parts of the supplement might differ from the article licence.

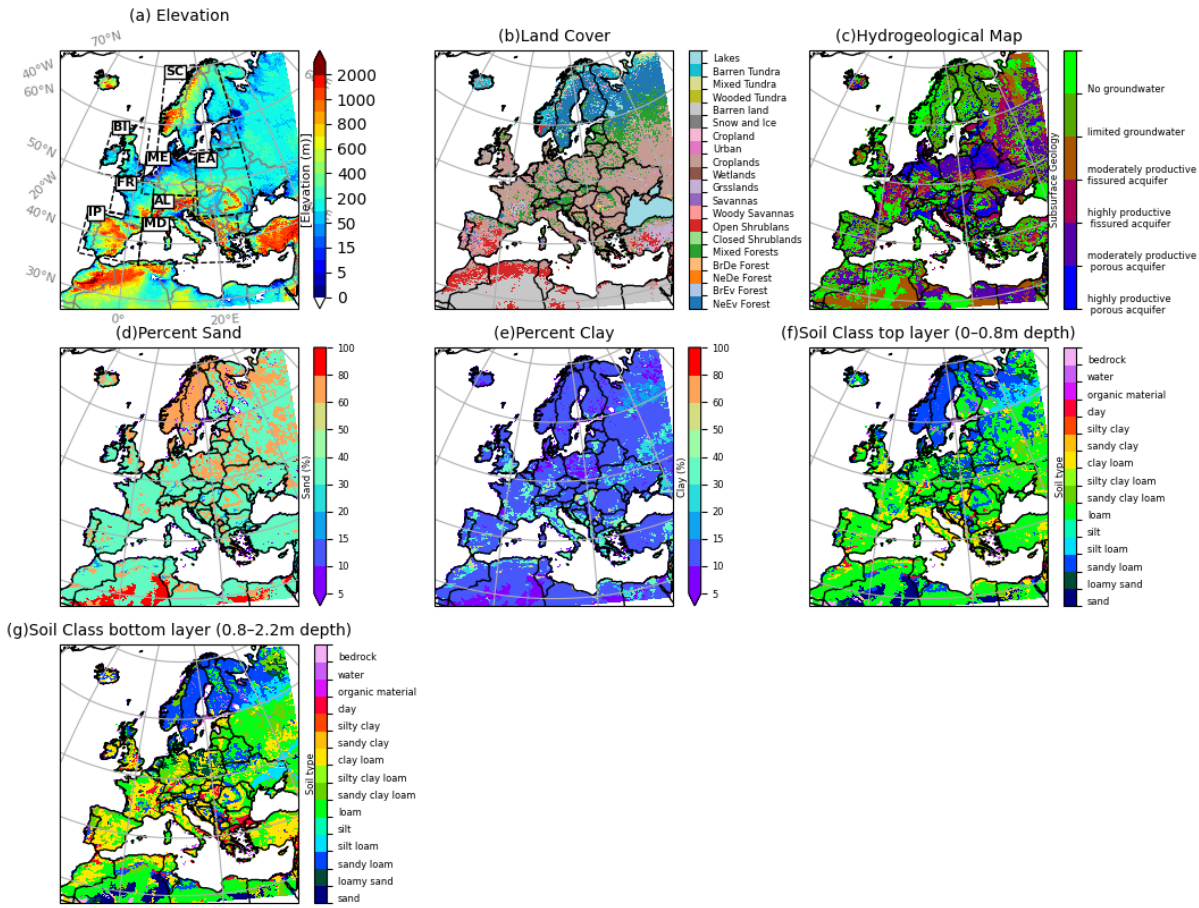


Figure S1: Model static fields input data: (a) elevation, b) dominant land use type based on MODIS data, (c)the upper layer of the subsurface geology plus the interconnected aquifer network, (d) percent sand content, (e) percent clay content based on global FAO soil database, (f) soil type classes used as upper layer, (g) soil type classes used for bottom layers in ParFlow model. The land use indices in (b) are defined as: 1:Evergreen Needleleaf Forest, 2:Evergreen Broadleaf Forest, 3:Deciduous Needleleaf Forest, 4:Deciduous Broadleaf Forest, 5:Mixed Forests, 6:Closed Shrublands, 7:Open Shrublands, 8: Woody Savannas, 9:Savannas, 10:Grasslands, 11:Permanent Wetlands, 12: Croplands, 13:Urban and Built-Up, 14: Cropland/Natural Vegetation Mosaic, 15: Snow and Ice, 16: Barren or Sparsely Vegetated,17: Water, 18:Wooded Tundra, 19:Mixed Tundra, 20:Barren Tundra, 21:Lakes. The inner boxes in (a) show the boundaries of the PRUDENCE regions (FR: France, ME: mid-Europe, SC: Scandinavia, EA: Eastern Europe, MD: Mediterranean, IP: Iberian Peninsula, BI: British Islands, AL: Alpine region; Christensen et al., 2007).

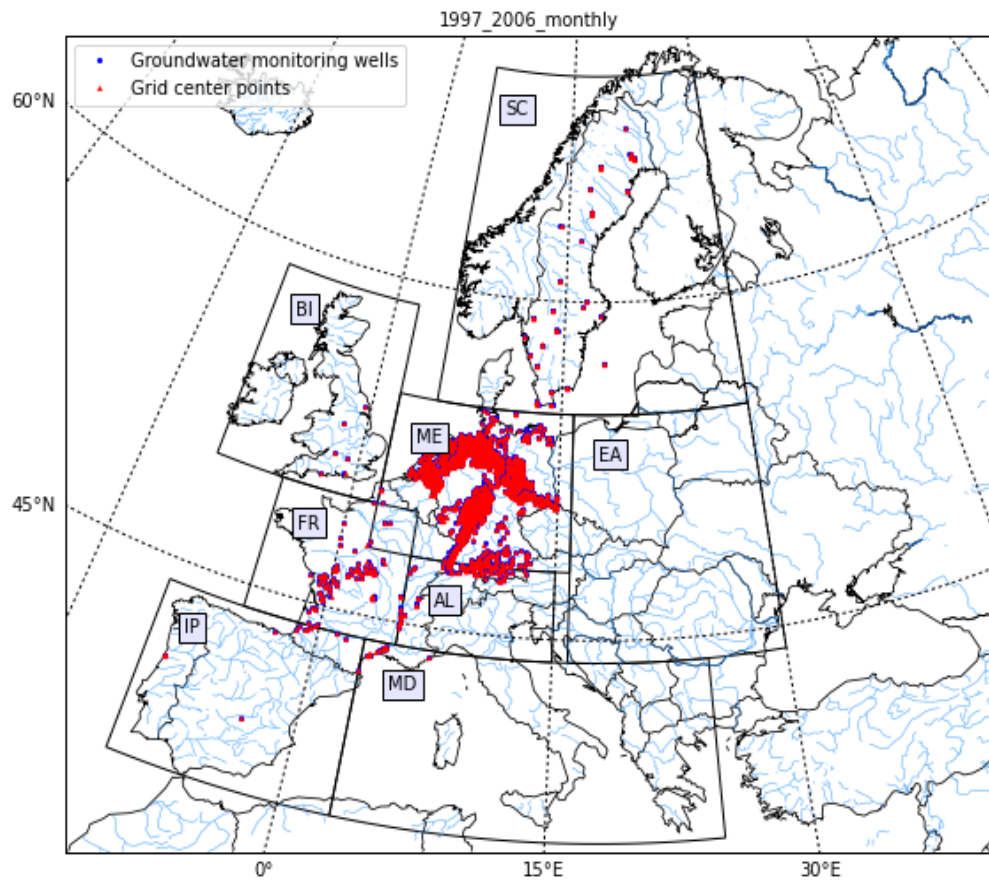


Figure S2: Location of the in situ water table depth data that were obtained through public web services or from the water management authorities in eight European countries. The WTD measurements were first converted to 3 km gridded WTD data by averaging WTD data from all the wells that lie within the same 3 km grid cell (displayed in red color).

Table S1: Detailed information of European GW monitoring wells applied in this study.

Country/region	Source	Number of GW monitoring wells
France	ADES (https://ades.eaufrance.fr/Recherche/Index/Piezometre?g=6b2839 , last access: June 2020)	219
Netherlands	DINOLoket (https://www.dinoloket.nl/en/subsurface-data , last access: June, 2020)	986
UK	British Geological Survey	6
Spain	Ministry for the Ecological Transition and the Demographic Challenge in Spain (https://sig.mapama.gob.es/redes-seguimiento/?herramienta=Piezometros , last access: July, 2020)	2

	2020)	
Portugal	National Information System for Hydrological Resources in Portugal (SNIRH) (https://snirh.apambiente.pt/index.php?idMain=2&idItem=1&objCover=100290946&objSite=2076000 , last access: July, 2020)	3
Sweden	Geological Survey of Sweden (SGU) (https://apps.sgu.se/kartvisare/kartvisare-grundvattenniva.html , last access: September, 2020)	78
Denmark	Geological Survey of Denmark and Greenland (GEUS) (https://data.geus.dk/geusmap/?mapname=jupiter&lang=en#baseMapDa&optlay=&extent=243844.8476598225.6148986.135096951.756963.341486983.6406933.6896236995&layers=jupiter_boringer_ws,jupiter_pejlinger&filter_0=dgunr%3D%26dybde.min%3D%26dybde.max%3D%26aar.min%3D%26aar.max%3D%26kode%3D , last access: August 2020)	4
Germany/Baden-Württemberg	Landesanstalt für Umwelt Baden-Württemberg (LUBW) (https://udo.lubw.baden-wuerttemberg.de/public/api/processingChain?ssid=324bd7d5-609d-4e8b-be1f-af7e073d56d5&selector=gwMessstellenauswahl.meros%3Amers_z_gw_messwerte_uis_gwstand_messstellen_refdb%24ind1.sel , last access: July, 2020)	475
Germany/Bavaria	Bayerisches Landesamt für Umwelt (https://www.gkd.bayern.de/en/groundwater/upper-layer/tables , last access: July, 2020)	102
Germany/Hessen	Hessisches Landesamt für Naturschutz, Umwelt und Geologie (http://lgd.hessen.de/mapapps/resources/apps/lgd/index.html?lang=en , last access: August, 2020)	653
Germany/Mecklenburg-Vorpommern/Middle Mecklenburg	Staatliches Amt für Landwirtschaft und Umwelt Mittleres Mecklenburg, Abteilung 4 Naturschutz, Wasser und Boden	11
Germany/Mecklenburg-Vorpommern/Vorpommern	Staatliches Amt für Landwirtschaft und Umwelt Vorpommern, Abteilung 4 - Naturschutz, Wasser und Boden, Dezernat 44 - Wasserrahmenrichtlinie, Gewässerkunde	24
Germany/Rhineland-Palatinate	Landesamt für Umwelt Rheinland-Pfalz (http://www.gdwasser.rlp.de/GDAWasser/client/gisclient/index.html?applicationId=12366&forcePreventCache=14143139175 , last access: August, 2020)	259
Germany/Saxony	Sächsisches Landesamt für Umwelt, Landwirtschaft und Geologie (https://www.umwelt.sachsen.de/umwelt/infosysteme/ida/pages/map/default/index.xhtml , last access: August, 2020)	720

Germany/Saxony-Anhalt	Landesbetrieb für Hochwasserschutz und Wasserwirtschaft des Landes Sachsen-Anhalt (LHW) (http://www.lhw.sachsen-anhalt.de/gld-portal , last access: August, 2020)	516
Germany/Schleswig-Holstein	Landesamt für Landwirtschaft, Umwelt und ländliche Räume des Landes Schleswig-Holstein (http://www.umweltdaten.landsh.de/atlas/script/index.php , last access: August, 2020)	55
Germany/Hamburg	Behörde für Umwelt, Klima, Energie und Agrarwirtschaft (BUKEA)	1
Germany/Lower Saxony	Niedersächsischen Landesdatenbank für wasserwirtschaftliche Daten (http://www.wasserdaten.niedersachsen.de)	961
Total		5075

Table S2: Summary of the ParFlow-CLM model performance for different variables and its comparison with CONUS implementation described by O'Neill et al. (2021)¹.

	This study (EU-CORDEX)			O'Neill et. al. 2021 (CONUS)			Comparison
Variable	Datasets used	R	pbias (%)	Datasets used	R	pbias (%)	
Streamflow	GRDC gauge stations (monthly)	0.77	-16 % (50th percentile)	USGS gauge stations (daily)	0.65 (50th percentile)	41.3 % (50th percentile)	PFCONUSv1: higher positive bias, EU-CORDEX: higher negative bias
ET	eddy covariance towers from FLUXNET dataset (daily)	0.94		eddy covariance towers from FLUXNET dataset (daily)	0.72 (50th percentile)	37.9% (50th percentile)	PFCONUSv1: positive bias EU-CORDEX: positive bias
	RS-based GLEAM and GLASS datasets (monthly)	0.91, 0.91 (50th percentile)	-9.9% and -18.2% (50th percentile)	RS MODIS dataset (MOD16A2) and SSEBop (monthly)	0.85 and 0.91 (50th percentile)	14.2% and 13.2% (50th percentile)	PFCONUSv1: Underpredicts ET in the north/east (wet/snow regions) and overpredicts in the south (dry regions). Underpredicts ET in the mountainous regions. EU-CORDEX: Underpredict ET in the wet/snow regions, small overpredictions in the south (dry regions). Underpredicts ET in the mountainous regions.
Soil Moisture	ESA-CCI (monthly)	0.70 (50th percentile)		ESA-CCI	0.69 (50th percentile)		PFCONUSv1: shows overall lower amplitude in the west (dry) and higher amplitude in the east (wet) relative to the CCI product; EU-CORDEX: overall wet bias, dry bias in southern Europe
TWS	GRACE dataset (monthly)	ranging from 0.76 and 0.91 for major regions		GRACE dataset (monthly)	ranging from 0.43 to 0.94 for major basins		Both model setups show stronger dry anomalies and overpredict wet anomalies relative to the GRACE data.
WTD	groundwater monitoring wells	0.50 (50th percentile)		groundwater monitoring wells	0.46 (50th percentile)		PFCONUSv1: a shallow WTD bias, EU-CORDEX: a shallow WTD bias

1: O'Neill, M. M. F., Tijerina, D. T., Condon, L. E., and Maxwell, R. M.: Assessment of the ParFlow–CLM CONUS 1.0 integrated hydrologic model: evaluation of hyper-resolution water balance components across the contiguous United States, Geosci. Model Dev., 14, 7223–7254,860 <https://doi.org/10.5194/gmd-14-7223-2021>, 2021.

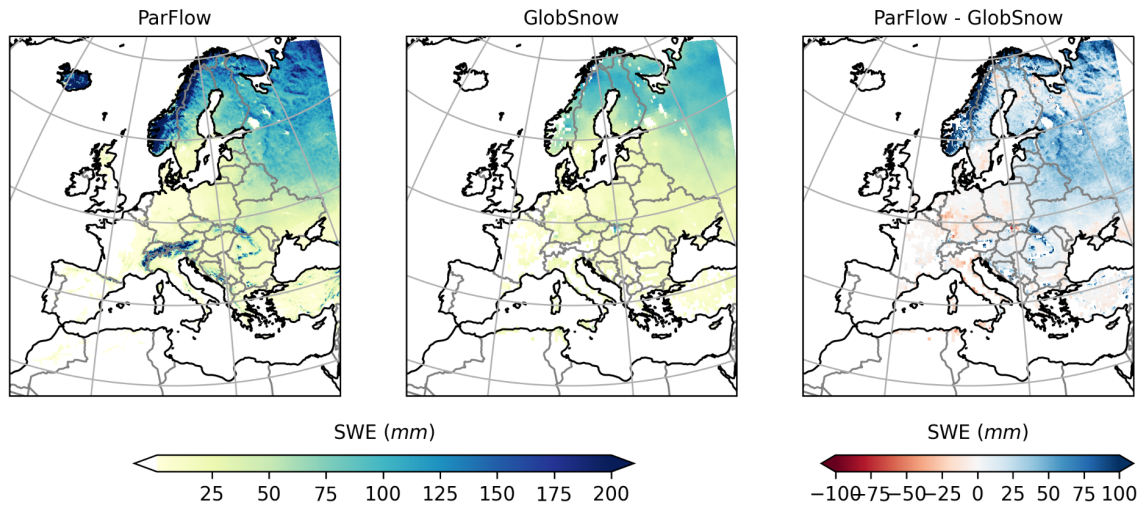


Figure S3: Comparison of time-averaged (1997-2006) ParFlow-CLM-simulated SWE for winter months (DJF) with the satellite-based ESA GlobSnow v3.0 estimated SWE (Luoju et al., 2021) over the non-mountainous areas of the 3 km EURO-CORDEX domain.

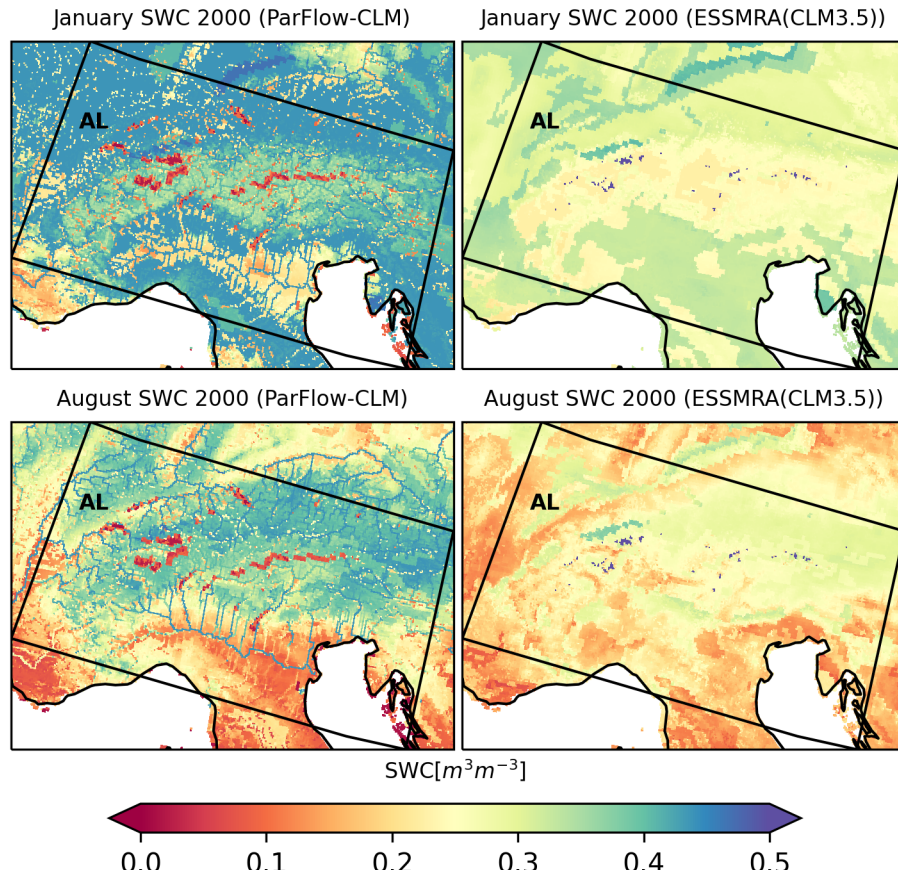


Figure S4. Spatial variability of surface soil moisture simulated by ParFlow-CLM and CLM3.5 at the surface soil layer for January and August months of year 2000 over the Alpine region. Note that glacier areas were not simulated by ParFlow-CLM and soil moisture values are zero at those grid cells.

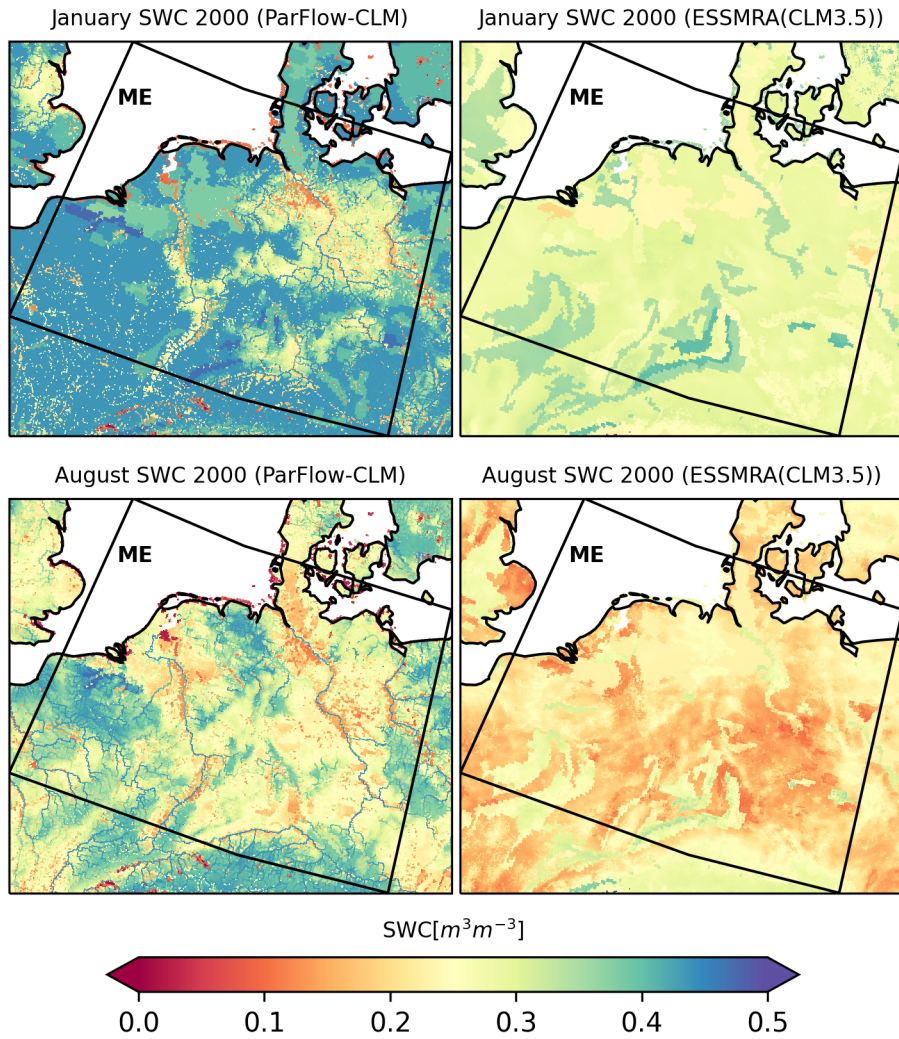


Figure S5. Spatial variability of surface soil moisture simulated by ParFlow-CLM and CLM3.5 at the surface soil layer for January and August months of year 2000 over the Mid-Europe region. Note that glacier areas were not simulated by ParFlow-CLM and soil moisture was set to zero.

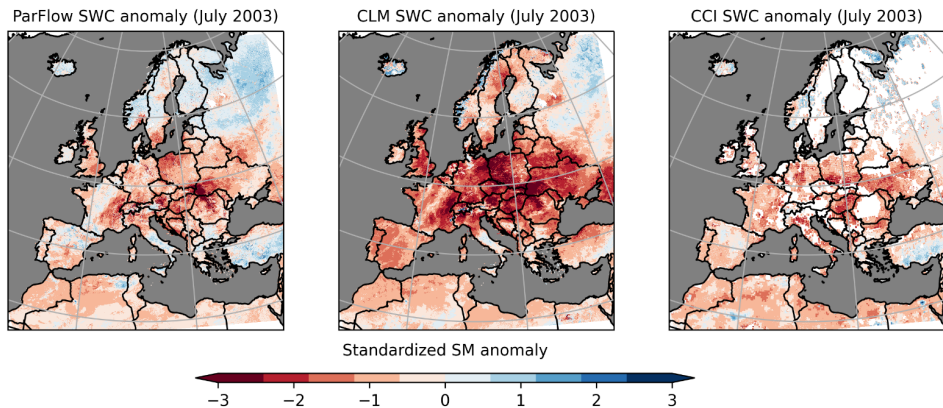


Figure S6: Comparison of surface soil moisture (SM) standardized anomaly for July, 2003 simulated by ParFlow-CLM with ESSMRA (CLM3.5) and ESA CCI datasets relative to the time period of 2000-2006.

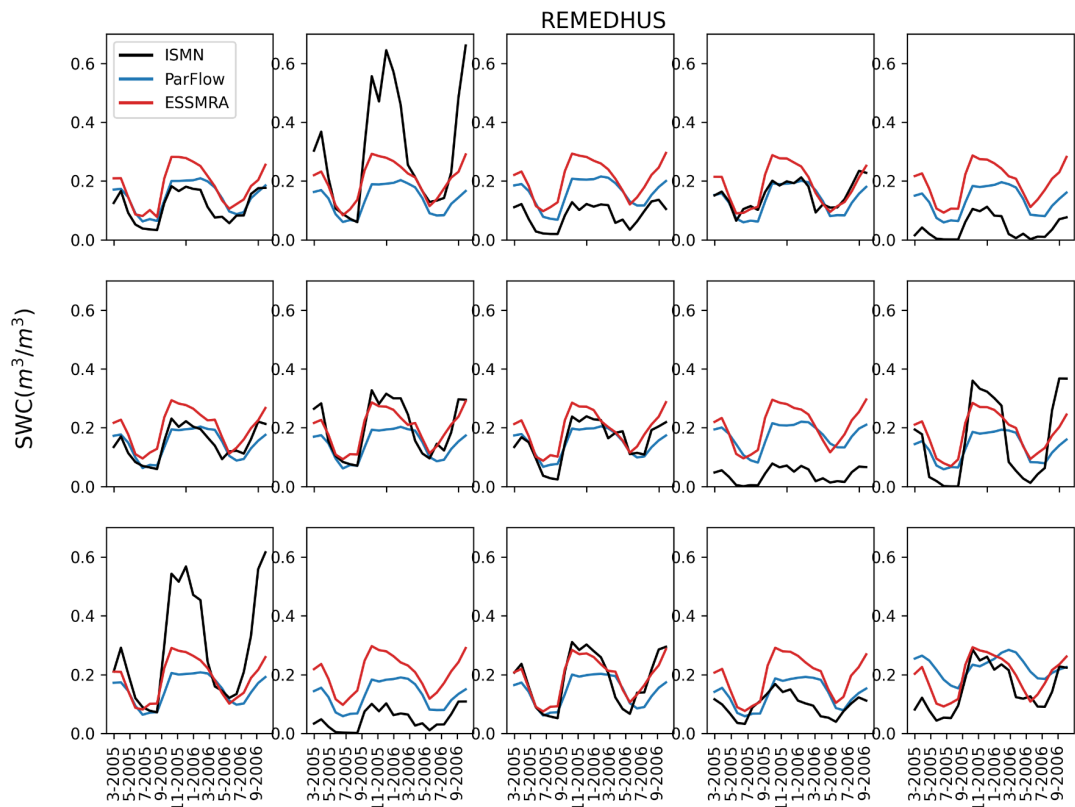


Figure S7: Comparison of monthly surface soil moisture estimated by ParFlow-CLM with ESSMRA (CLM3.5) for in situ stations located in the REMEDHUS network in Spain. The comparison was only made for months when observations were available within the 2000-2006 period.

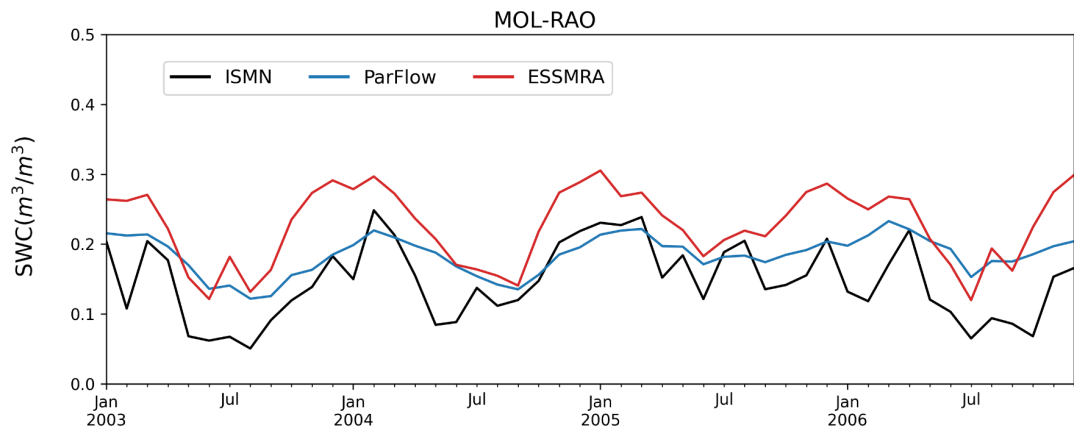


Figure S8: Same as Figure S5, but for in situ stations located in the MOL-RAO network in Germany.

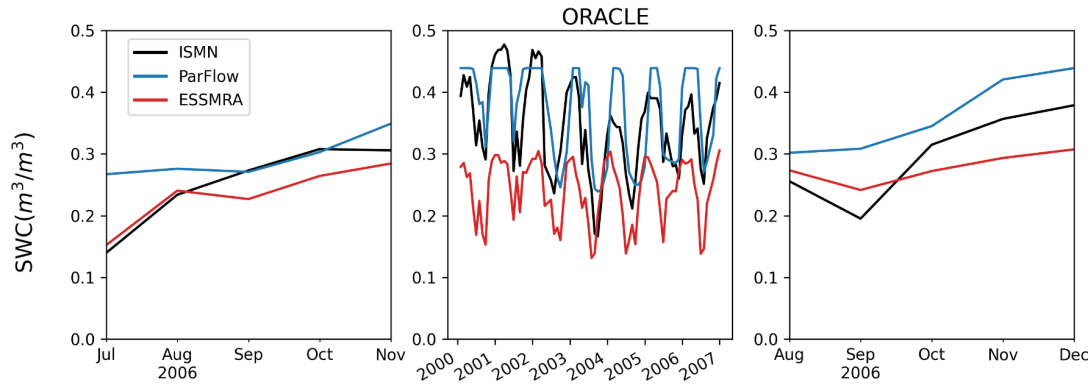


Figure S9: Same as Figure S5, but for in situ stations located in the ORACLE network in France.

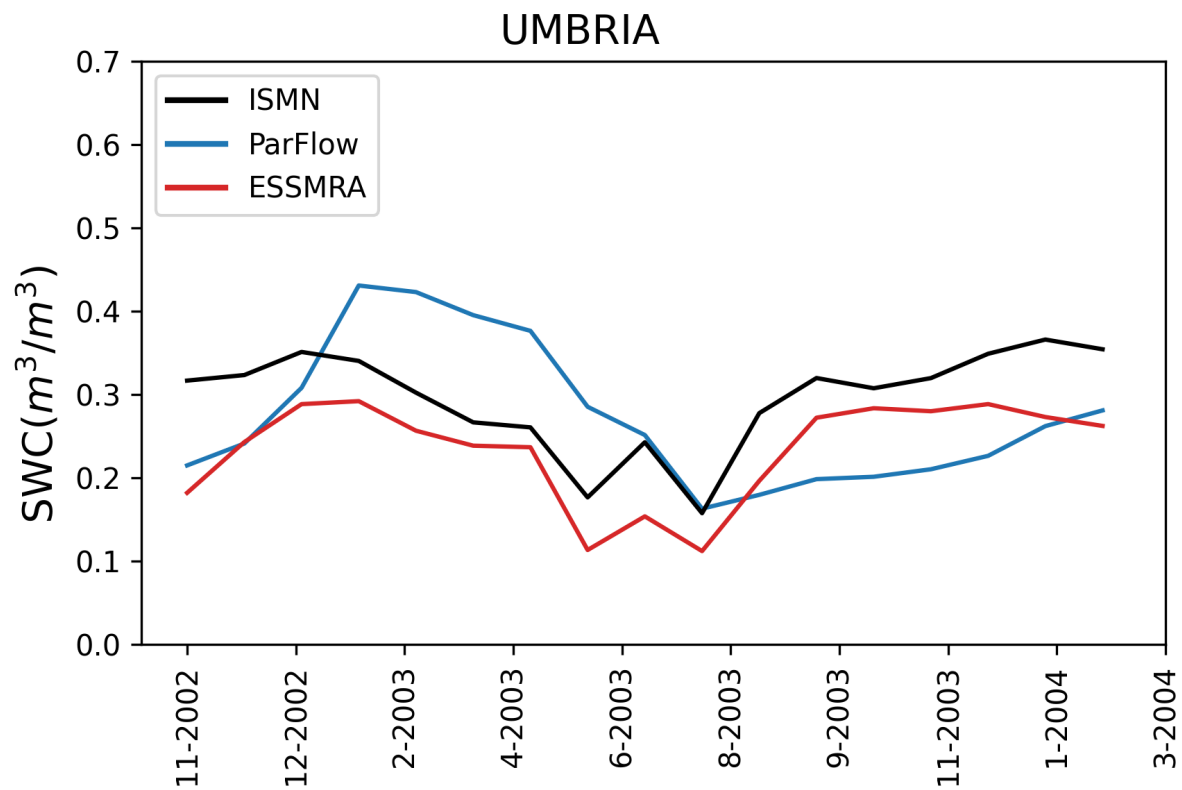


Figure S10: Same as Figure S5, but for in situ stations located in UMBRIA network in Italy.

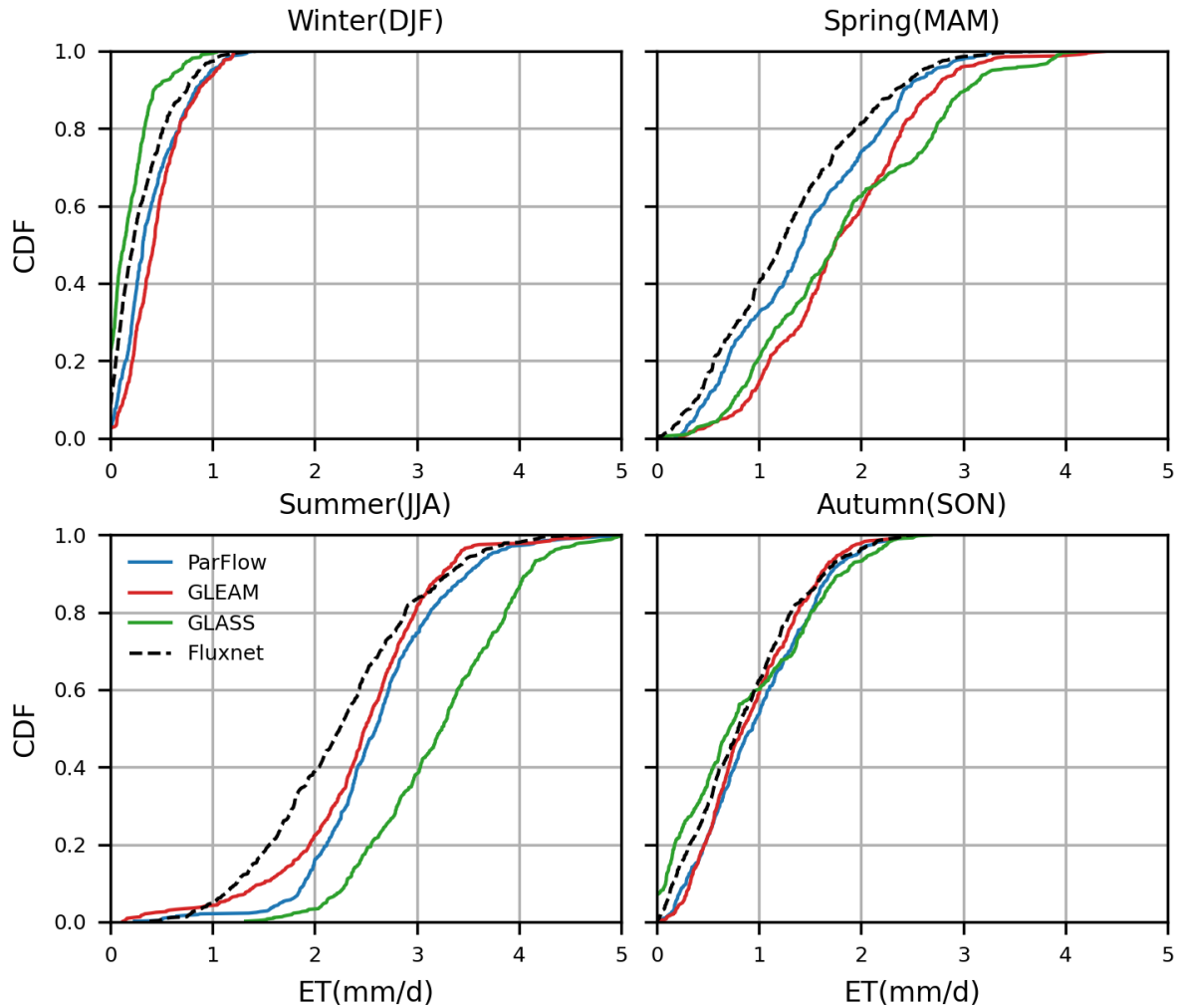


Figure S11: Evaluation of ParFlow-CLM-simulated monthly evapotranspiration (ET) with ground-based observations and with GLEAM and GLASS datasets at 60 eddy-covariance FLUXNET stations.

Table S3: Comparison of seasonal average ET estimated by ParFlow-CLM with GLEAM and GLASS datasets over PRUDENCE regions.

	ParFlow-CLM				GLEAM				GLASS			
Regions	DJF (mm/d)	MAM (mm/d)	JJA (mm/d)	SON (mm/d)	DJF (mm/d)	MAM (mm/d)	JJA (mm/d)	SON (mm/d)	DJF (mm/d)	MAM (mm/d)	JJA (mm/d)	SON (mm/d)
BI	0.43	1.31	2.07	0.86	0.42	1.68	2.25	0.81	-0.01	1.64	2.79	0.54
IP	0.54	1.61	2.02	1.02	0.76	2.16	1.92	1.03	0.64	2.46	3.42	1.37
FR	0.38	1.67	2.79	1.02	0.52	1.96	2.61	1.01	0.27	2.14	3.51	1.00
ME	0.25	1.43	2.59	0.81	0.40	1.73	2.45	0.81	0.13	1.82	3.19	0.75
SC	0.21	0.79	2.02	0.58	0.10	1.28	2.38	0.57	-0.07	0.99	2.48	0.23
AL	0.33	1.40	2.72	0.97	0.58	1.94	2.86	1.19	0.26	1.76	3.27	0.96
MD	0.51	1.73	2.44	1.10	0.73	2.26	2.37	1.12	0.52	2.35	3.54	1.30
EA	0.15	1.40	2.71	0.79	0.32	1.73	2.52	0.82	0.14	1.76	3.27	0.79
Average	0.35	1.42	2.42	0.89	0.48	1.84	2.42	0.92	0.23	1.86	3.19	0.87

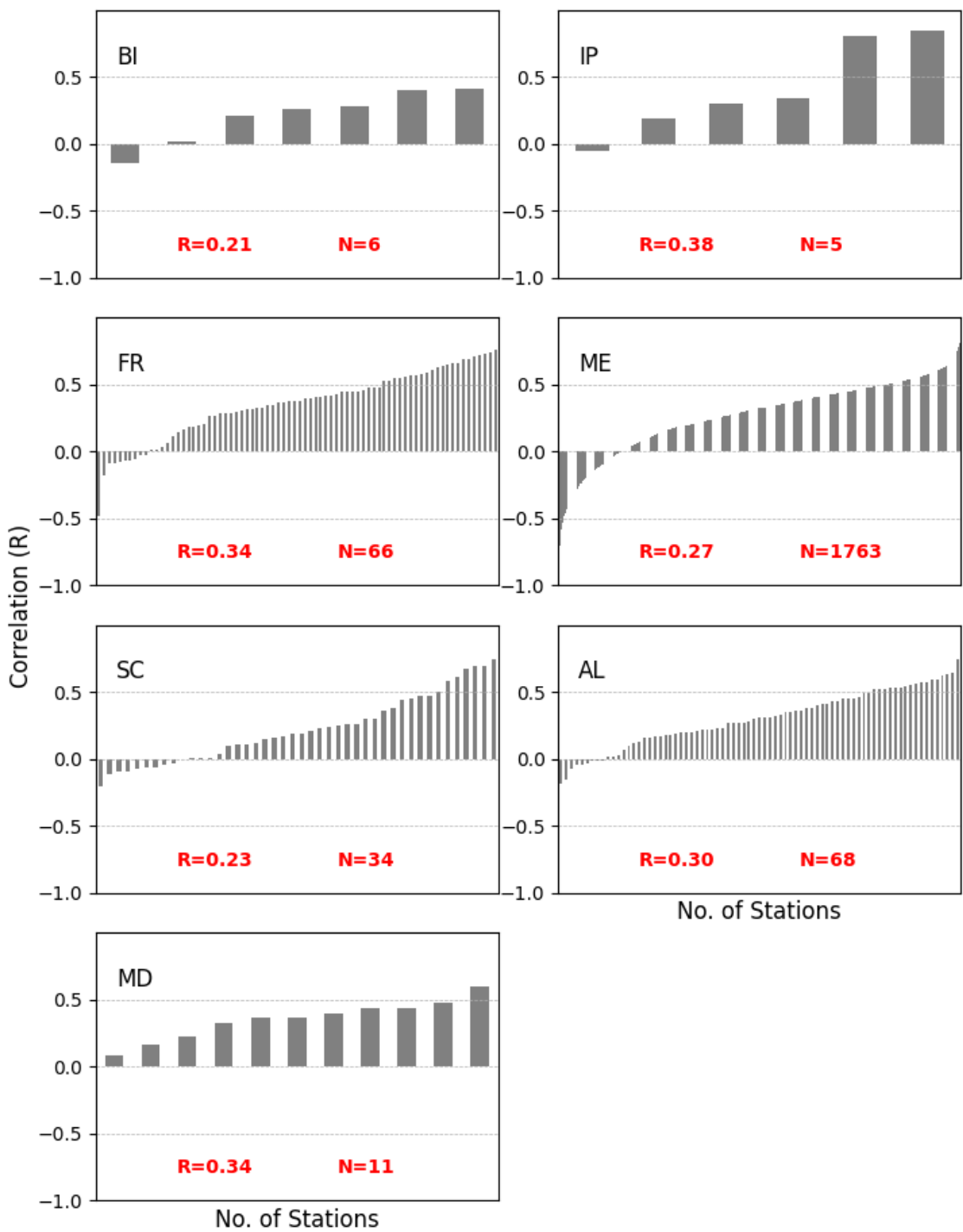


Figure S12: Correlation of ParFlow-CLM-simulated WTD anomalies with observed WTD anomalies for the time period of 1997-2006 for individual stations within PRUDENCE regions. N indicates number of gridcells where groundwater wells are located within each region.

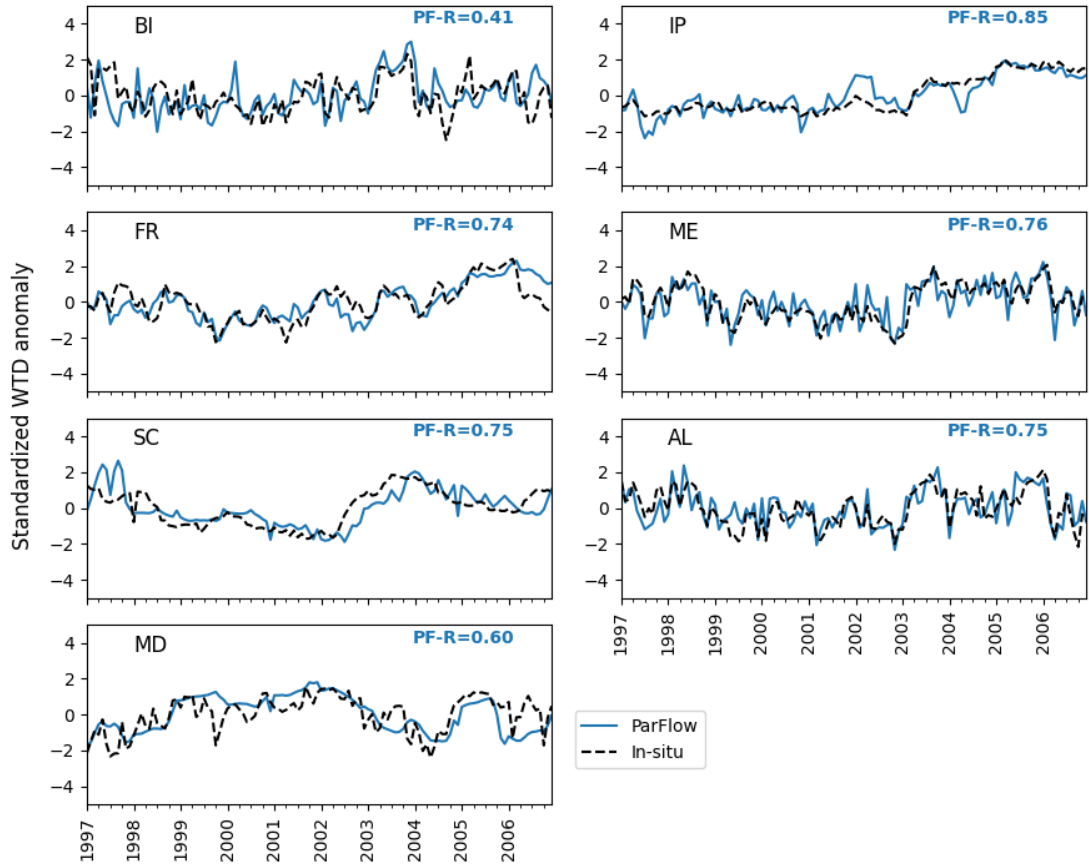


Figure S13: Comparison of ParFlow-CLM-simulated WTD anomalies with observed WTD for selected grid cells with highest correlation values in each PRUDENCE region.

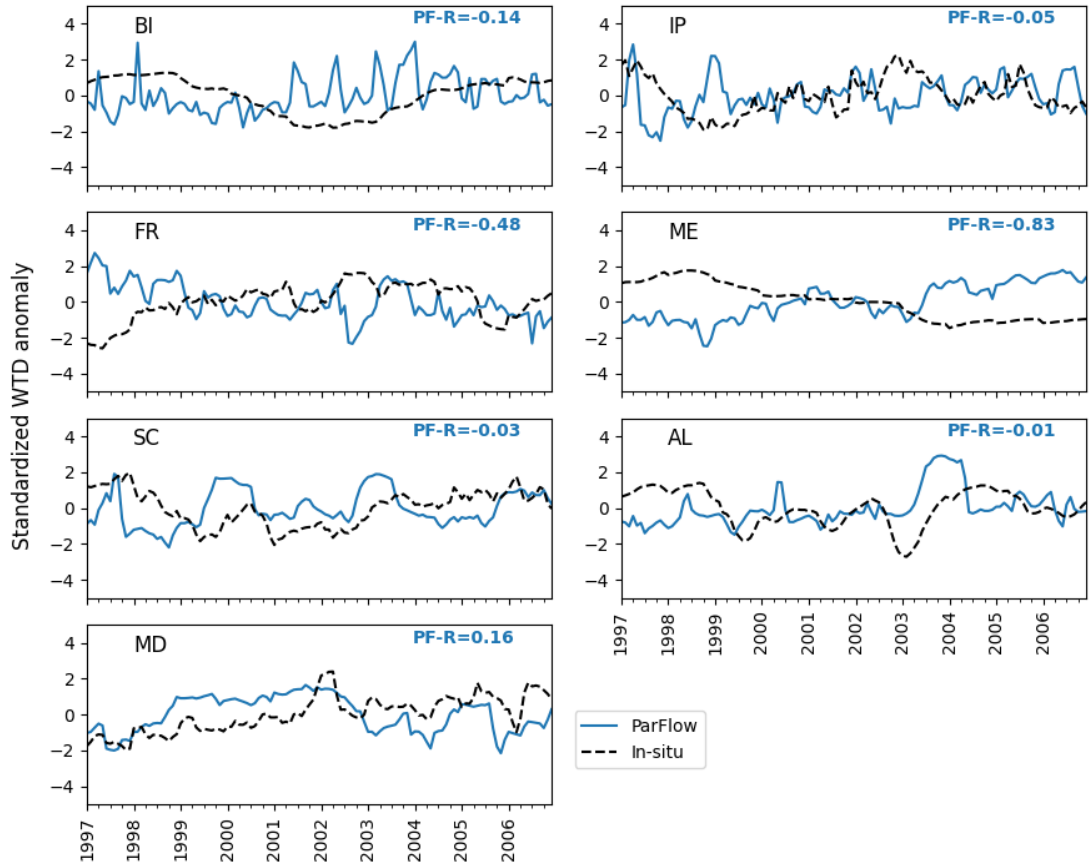


Figure S12: Comparison of ParFlow-CLM-simulated WTD anomalies with observed WTD for selected grid cells with lowest correlation values in each PRUDENCE region.